JOURNAL OF SOLID STATE CHEMISTRY **122,** 266–272 (1996)
ARTICLE NO. 0112

Crystal Structure and Magnetism of Ternary Compounds RE_6MSb_{15}, RE = La, Ce and M = Mn, Cu, Zn

O. Sologub, M. Vybornov, P. Rogl, and K. Hiebl

Institut für Physikalische Chemie der Universität Wien, A-1090 Wien, Währingerstraße 42, Austria

and

G. Cordier and P. Woll

Anorganische Chemie II, Eduard Zintl Institut, Technische Hochschule Darmstadt, D-64289 Darmstadt, Germany

Received April 4, 1995; in revised form December 1, 1995; accepted December 5, 1995

A series of novel ternary compounds RE_6MSb_{15} has been synthesized (a) via arc melting elemental metal ingots (M = Mn or Cu) or (b) via reaction sintering cold compacted powder blends (M = Zn). The crystal structure was solved for La_6MnSb_{15} from single crystal X-ray counter data (La_6MnSb_{15}-type, $Imm2$, $Z = 2$, $a = 1.5376$, $b = 1.9611$, $c = 0.4314$ nm, $R_F = 0.067$ for 923 reflections ($|F_0| > 3\sigma$)). The Rietveld refinement of the crystal structure of Ce_6MnSb_{15} using Cu$K\alpha$-X-ray data from a D5000 Siemens diffractometer confirmed atom order and crystal symmetry $Imm2$ ($R_I = 0.049$, $R_F = 0.031$) and revealed small deficiencies in the Mn site as well as for one of the Sb sites. Employing X-ray powder Guinier techniques the new compounds were all found to be isostructural with the La_6MnSb_{15} type. Magnetic measurements performed down to liquid helium temperature give evidence that both compounds Ce_6MnSb_{15} and Gd_6ZnSb_{15} undergo an antiferromagnetic transition at 7 and 15 K, respectively. Ce_6ZnSb_{15} and Pr_6ZnSb_{15} remain paramagnetic in the temperature range investigated, whereas Sm_6ZnSb_{15} is a Van-Vleck-type paramagnet. © 1996 Academic Press, Inc.

INTRODUCTION

Our interest in the magnetic potential of ternary cerium (neodymium)–manganese–metametal alloys has prompted us to investigate the phase relations in an isothermal section of the Ce(Nd)–Mn–Sb systems at 600°C (1). One of the three ternary compounds discovered in the Ce(Nd)–Mn–Sb systems revealed a chemical formula close to $RE_{\sim 6}Mn_{\sim 1}Sb_{\sim 15}$. Composition and X-ray powder intensities closely resembled that of the homologous compound La_6MnSb_{15} earlier reported by one of us (2, 3). Whereas only the La-containing phases La_6MnSb_{15} with M = Cu, Zn have been pursued earlier (2, 3), a detailed inspection of isotypic representatives RE_6MSb_{15} among the light rare earth elements and M = Mn, Cu, Zn became the subject of the present work emphasizing on their formation, crystal structure, and magnetic behavior.

EXPERIMENTAL

The compounds Ce_6MSb_{15} (M = Mn, Cu), each with a total amount of ca. 1 g were prepared by argon arc melting from ingots of the high purity elements obtained from Johnson Matthey and Co., UK (99.9 mass%). The manganese platelets were surface cleaned in dilute HNO_3 prior to use. Weight losses due to vaporization while melting were less than 2 mass% and were compensated beforehand by extra amounts of Mn and Sb. The arc melted buttons were then annealed at 600°C in vacuum-sealed quartz capillaries for 170 h and finally quenched by submerging the capsules into cold water.

Due to the generally high vapor pressure of zinc at elevated temperatures, the zinc containing compounds RE_6ZnSb_{15}, RE = Ce, Pr, Nd, Sm, and Gd, were synthesized by repeated reaction sintering of stoichiometric amounts of rare earth filings (Auer Remy, ingots of 99.9 mass%), and powders of zinc (Merck, 99.8%) and antimony (Johnson Matthey and Co., UK, 99.5 mass%). Proper powder blends were compacted into small pellets in a 6-mm diameter steel die without the use of lubricants, sealed in evacuated quartz tubes and within 100 h slowly heated to the annealing temperature of 600°C.

Despite that the products were found to be remarkably stable in dry as well as moist air, handling of the materials during the individual steps of preparation in an argon filled glove box system with controlled atmosphere (<3 ppm O_2 and <5 ppm H_2O) is recommended.

Lattice parameters and standard deviations (see Table 1) were obtained by least squares refinements of room

0022-4596/96 $18.00
Copyright © 1996 by Academic Press, Inc.
All rights of reproduction in any form reserved.

TABLE 1
Crystallographic and Magnetic Data of Ternary Compounds RE_6MSb_{15}, M = Mn, Cu, Zn; La_6MnSb_{15}-Type

Compound	Lattice parameters (nm)			V	T_N	Θ_P	$\mu_{eff.}^{meas.}$	$\mu_{eff./RE}^{theor.}$	Ref.
	a	b	c	(nm^3)	(K)	(K)	(μ_B)	(μ_B)	
La_6MnSb_{15}	1.5376(5)	1.9611(6)	0.4314(2)	1.3008					2
Ce_6MnSb_{15}	1.5161(4)	1.9371(6)	0.42754(9)	1.2555	7	−6	8.9	2.54	*
La_6CuSb_{15}	1.5395(8)	1.9465(8)	0.4333(4)	1.3017					3
Ce_6CuSb_{15}	1.5452(6)	1.9178(7)	0.4378(2)	1.2974					*
La_6ZnSb_{15}	1.5430(5)	1.9461(6)	0.4351(2)	1.3065					2
Ce_6ZnSb_{15}	1.5215(2)	1.9264(6)	0.43215(5)	1.2667	—	−10	2.7	2.54	*
Pr_6ZnSb_{15}	1.5136(4)	1.9180(5)	0.42898(5)	1.2453	—	−13	3.6	3.6	*
Nd_6ZnSb_{15}	1.5109(6)	1.9026(9)	0.42447(7)	1.2201					*
Sm_6ZnSb_{15}	1.5004(3)	1.8794(6)	0.41769(9)	1.1778	—	9	0.5	—	*
Gd_6ZnSb_{15}	1.4942(6)	1.8740(7)	0.41528(11)	1.1628	15	−34	7.7	7.9	*

Note. Space group $Imm2$, C_{2v}^{20}, No. 44, origin on $mm2$, $Z = 2$, lattice parameter data as obtained from Guinier.

temperature Guinier–Huber X-ray powder data using monochromatic Cu$K\alpha_1$ radiation and an internal standard of 99.9999% pure Ge ($a_{Ge} = 0.5657906$ nm). A full profile full matrix Rietveld refinement was performed on a flat specimen powder sample of Ce_6MnSb_{15} with Cu$K\alpha$ radiation in a D5000 Siemens diffractometer equipped with a secondary monochromator. Preferred orientation effects were minimized by powdering the sample to a grain size smaller than 15 μm in a WC-Co and an agate mortar.

Single crystals of La_6MSb_{15} (M = Mn, Zn, Cu) were grown of melts of the nominal composition $LaM_{0.25}Sb_2$ (La 99.6 mass%, Alfa; Mn 99.9 mass%, Merck; Zn p.a., Merck; Cu 99.5 mass%, Merck; total amount ca. 5 g). The samples were heated in corundum crucibles in argon atmosphere to temperatures of 1230°C and cooled to room temperature with a rate of 100 K/h.

Magnetic data were recorded in the range $4.2 < T < 100$ K in a Lakeshore a.c. susceptometer. For measurements from 80 to 550 K a compensating high precision Faraday pendulum SUS10 in external fields up to 1.3 Tesla was used.

RESULTS AND DISCUSSION

A. Structural Chemistry

A.1. Crystal structure determination of La_6CuSb_{15}, La_6ZnSb_{15} and La_6MnSb_{15}. Precession and Weißenberg photographs (Mo$K\alpha$, graphite monochromator) of single crystals of La_6MnSb_{15} showed a body-centered cell of orthorhombic symmetry. No hints of additional reflections could be found. To determine the crystal structures, the intensities of the reflections of La_6CuSb_{15} and La_6ZnSb_{15} were measured by an automatic two-circle diffractometer STOE-STADI 2; the intensities of the reflections of La_6MnSb_{15} were determined by a Philips PW1100 four-circle diffractometer (Mo$K\alpha$, graphite monochromator, Table 2). Polarization, Lorentz, and absorption corrections were applied. A first structure model was derived in the centrosymmetric space group $Immm$ by direct methods combined with additional Fourier and difference Fourier syntheses, but led to extremely short distances for Sb–Sb arising due to the mirror plane perpendicular to the c axis. In the space group $Imm2$, however, the position $4j$ ((1/2, 0, z) $Immm$) after standardization can be split into two positions, $2b$ (0 1/2 z) = $2a$ (00z (i.e., Sb_6)), of which only one is occupied. Extremely high values in the displacement factors suggested the refinement of the occupation factors of the transition elements (Mn, Zn, and Cu), resulting in a half occupation. During the refinements in the space group $Imm2$ the z parameters did not significantly move from the positions at $z = 0$ with the exception of those of the atoms Sb6 which are violating the centrosymmetric symmetry. The resulting pseudosymmetric crystal structure enforced refinement of positional parameters using the symmetry restrictions of the centrosymmetric space group $Immm$ (i.e., fixing these parameters at $z = 0$, but allowing refinement of the thermal parameters on the other hand).

A.2. Rietveld refinement of the crystal structure of Ce_6MnSb_{15}. RT-Rietveld full matrix full profile refinement of the X-ray powder data of Ce_6MnSb_{15} based on the structure model of La_6MnSb_{15} confirms atom order and site occupation in the orthorhombic noncentrosymmetric space group $Imm2$ as earlier derived from an X-ray single crystal counter study for the homologous phases La_6MSb_{15}, M = Mn, Cu, Zn, and thereby proves isotypism with the structure type of La_6MnSb_{15} (see above). In accordance with the results obtained from the investigation of the phase relations in the Ce–Mn–Sb system, there is a significant deficiency on the Mn site as well as a minor defect for the Sb5 sites resulting in a more correct formula

TABLE 2
Structural Data for La_6MnSb_{15}, La_6CuSb_{15}, La_6ZnSb_{15}, and Ce_6MnSb_{15}
(Standard Deviations in Parenthesis)

Parameter	La_6MnSb_{15}	La_6CuSb_{15}	La_6ZnSb_{15}	Ce_6MnSb_{15}
a (nm)	1.5376(5)	1.5395(8)	1.5430(5)	1.51538(2)
b (nm)	1.9611(6)	1.9465(8)	1.9461(6)	1.93646(3)
c (nm)	0.4314(2)	0.4333(4)	0.4351(2)	0.427422(7)
Volume (nm^3)	1.3008	1.2984	1.3065	1.2543
Density (Mg/m^3) (exp)	6.93	6.95	6.93	7.18 (calc)
Crystal system	Orthorhombic			
Space group	*Imm*2 (No. 44), origin at *mm*2			
Z	2			
Data collection				
Diffractometer	PHILIPS PW1100 Mo$K\alpha$	STOE STADI Mo$K\alpha$	STOE STADI Mo$K\alpha$	SIEMENS D5000 Cu$K\alpha$
Reflections meas., $8° \le 2\theta \le 60°$, (symmetry independent)	2728 (1130)	2078 (1051)	1978 (1029)	
Reflections for refinement, $\ge 3\sigma$)	923	965	919	570 ($20° \le 2\theta \le 115°$)
μ (mm^{-1})	25.66	25.98	25.99	24.68
$R_F = \Sigma\lvert F_o - F_c\rvert/\Sigma F_o$	0.067	0.095	0.064	0.031
$R_I = \Sigma\lvert I_{oB} - I_{cB}\rvert/\Sigma I_{oB}$				0.049
$R_{wP} = (\Sigma w_i(y_{oi} - y_{ci})^2/\Sigma w_i y_{oi}^2)^{1/2}$				0.085
$R_P = \Sigma\lvert y_{oi} - y_{ci}\rvert/\Sigma\lvert y_{oi}\rvert$				0.065
$R_e = \{(N - P + C)/\Sigma w_i y_{oi}\}^{1/2}$				0.042
$S = R_{wP}/R_e$				2.01
Refinement	SHELXL-76	SHELXL-76	SHELXL-76	RIETVELD
Atom parameters	La_6MnSb_{15}	La_6CuSb_{15}	La_6ZnSb_{15}	Ce_6MnSb_{15}
8 La1 (Ce1) on 8*e* (x y 0)				
x	0.1393(1)	0.1395(2)	0.1389(1)	0.1408(2)
y	0.1339(1)	0.1338(1)	0.1353(1)	0.1322(1)
z	0.0894	0.0701	0.1049	0.0787
$B_{eq}(B_{iso})\cdot 10^2$ (nm^2)	0.11(1)	0.23(2)	0.13(1)	0.25(6)
4 La2 (Ce2) on 4*d* (0 y z)				
y	0.3234(1)	0.3254(2)	0.3270(1)	0.3232(2)
z	0.0894	0.0701	0.1049	0.0787
$B_{eq}(B_{iso})\cdot 10^2$ (nm^2)	0.16(21)	0.25(21)	0.19(3)	0.20(9)
2 Mn (Cu, Zn) on 4*c* (x 0 z)				
x	0.2772(13)	0.2606(12)	0.2590(8)	0.2751(18)
z	0.0894	0.0701	0.1049	0.0787
$B_{eq}(B_{iso})\cdot 10^2$ (nm^2)	0.50(8)	0.56(7)	0.41(5)	0.88(7)
8 Sb1 on 8*e*(x y z)				
x	0.2148(1)	0.2144(1)	0.2146(1)	0.2139(2)
y	0.2973(1)	0.2981(1)	0.2984(1)	0.2979(1)
z	0.0894	0.0701	0.1049	0.0787
$B_{eq}(B_{iso})\cdot 10^2$ (nm^2)	0.68(5)	0.51(5)	0.73(4)	0.14(3)
8 Sb2 on 8*e*(x y z)				
x	0.3586(2)	0.3557(2)	0.3561(1)	0.3595(2)
y	0.1075(2)	0.1074(1)	0.1070(1)	0.1062(1)
z	0.0894	0.0701	0.1049	0.0787
$B_{eq}(B_{iso})\cdot 10^2$ (nm^2)	0.38(2)	0.21(2)	0.29(2)	0.91(1)
4 Sb3 on 4*d*(0 y z)				
y	0.1972(2)	0.1995(2)	0.2006(1)	0.1968(2)
z	0.5894	0.5701	0.6049	0.5787
$B_{eq}(B_{iso})\cdot 10^2$ (nm^2)	0.14(2)	0.25(3)	0.18(2)	0.05(3)
4 Sb4 on 4*c*(x 0 z)				
x	0.1568(3)	0.1559(3)	0.1535(2)	0.1603(3)
z	0.5894	0.5701	0.6049	0.5787
$B_{eq}(B_{iso})\cdot 10^2$ (nm^2)	0.30(2)	0.32(3)	0.34(3)	0.40(3)

TABLE 2—*Continued*

Parameter	La_6MnSb_{15}	La_6CuSb_{15}	La_6ZnSb_{15}	Ce_6MnSb_{15}
4 Sb5 on 4*c* (*x* 0 *z*)				
x	0.4063(4)	0.4054(4)	0.4083(3)	0.4066(4)
z	0.5894	0.5701	0.6049	0.5787
$B_{eq}(B_{iso})\cdot 10^2$ (nm^2)	0.69(4)	0.51(4)	0.51(3)	0.9(2)
2 Sb6 on 2a (0 0 *z*)				
z	0.0000(17)	0.0000(21)	0.0000(17)	0.0000(19)
$B_{eq}(B_{iso})\cdot 10^2$ (nm^2)	0.25(4)	0.42(7)	0.307(4)	0.9(2)

Distances [nm] within the first nearest neighbor coordination (standard deviations are in all cases smaller than $\sigma \leq 0.0015$)

	La_6MnSb_{15}	La_6CuSb_{15}	La_6ZnSb_{15}	Ce_6MnSb_{15}	Multip.	CN
*RE*1–*M*	0.3375	0.3203	0.3220	0.3270		10
–Sb3	0.3283	0.3305	0.3307	0.3269	2	
–Sb1	0.3392	0.3396	0.3393	0.3354	2	
–Sb1	0.3408	0.3400	0.3381	0.3395		
–Sb4	0.3409	0.3400	0.3423	0.3348	2	
–Sb6	0.3410	0.3389	0.3426	0.3350		
–Sb2	0.3412	0.3368	0.3396	0.3352		
*RE*2–Sb3	0.3283	0.3274	0.3284	0.3249	2	10
–Sb1	0.3343	0.3343	0.3357	0.3278	2	
–Sb2	0.3349	0.3371	0.3364	0.3312	4	
–Sb5	0.3751	0.3698	0.3652	0.3705	2	
M –Sb2	0.2451	0.2553	0.2565	0.2422	2	8
–Sb4	0.2843	0.2704	0.2717	0.2756	2	
–Sb5	0.2941	0.3113	0.3169	0.2922	2	
–*RE*1	0.3375	0.3203	0.3220	0.3270	2	
Sb1 –Sb2	0.3069	0.3043	0.3051	0.3042	2	8
–Sb1	0.3043	0.3070	0.3078	0.3034	2	
–*RE*2	0.3343	0.3343	0.3357	0.3278		
–*RE*1	0.3392	0.3396	0.3393	0.3354	2	
–*RE*1	0.3408	0.3400	0.3381	0.3395		
Sb2 –*M*	0.2451	0.2553	0.2565	0.2422		8
–Sb1	0.3079	0.3043	0.3051	0.3042	2	
–Sb5	0.3103	0.3111	0.3117	0.3051	2	
–*RE*2	0.3349	0.3371	0.3364	0.3312	2	
–*RE*1	0.3412	0.3368	0.3396	0.3352		
Sb3 –*RE*2	0.3283	0.3274	0.3284	0.3249	2	6
–*RE*1	0.3283	0.3312	0.3307	0.3269	4	
Sb4 –*M*	0.2843	0.2704	0.2717	0.2756	2	8
–Sb6	0.2992	0.3041	0.2927	0.3024		
–*RE*1	0.3409	0.3401	0.3423	0.3348	4	
–Sb6	0.3504	0.3449	0.3541	0.3467		
Sb5 –Sb5	0.2882	0.2911	0.2831	0.2831		9
–Sb2	0.3103	0.3111	0.3117	0.3051	4	
–*M*	0.2931	0.3113	0.3169	0.2922	2	
–*RE*2	0.3751	0.3698	0.3652	0.3705	2	
Sb6 –Sb4	0.2992	0.3041	0.2927	0.3024	2	8
–*RE*1	0.3410	0.3389	0.3426	0.3350	4	
–Sb4	0.3504	0.3449	0.3540	0.3467	2	

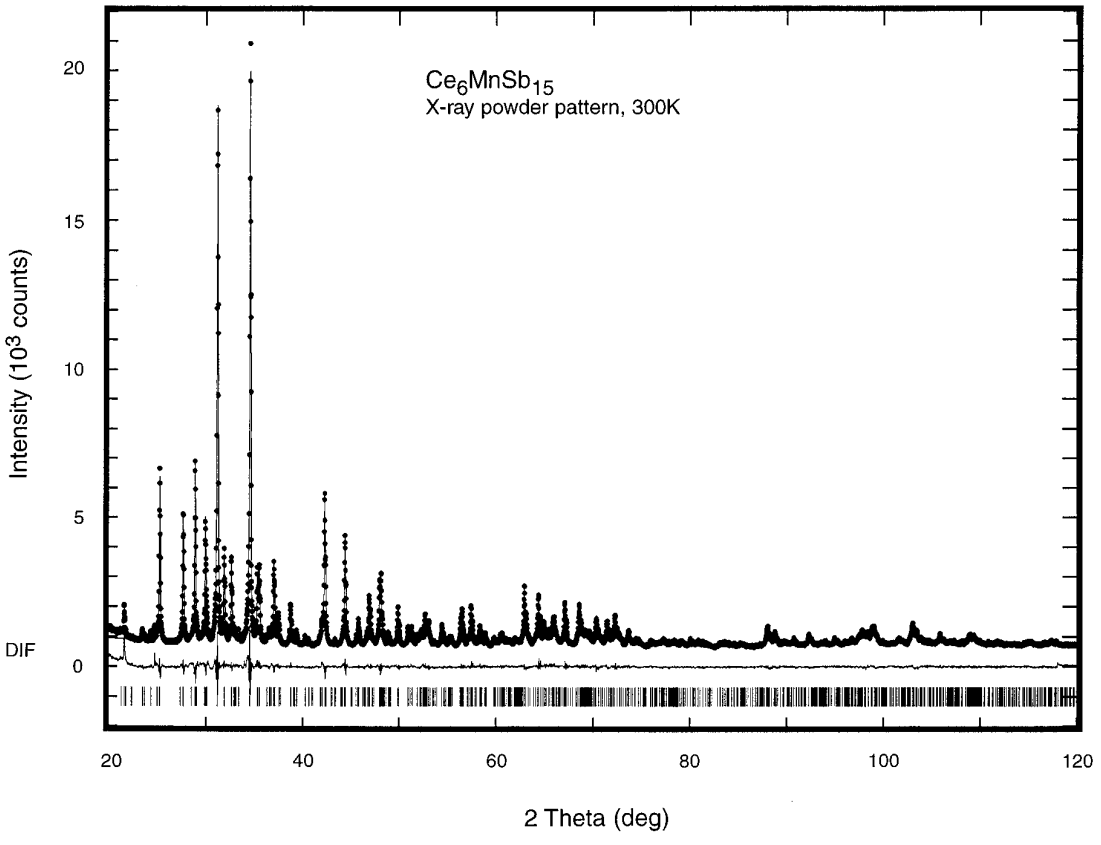

FIG. 1. Comparison of observed and calculated (Rietveld refinement) X-ray powder profiles of Ce_6MnSb_{15}.

$Ce_6Mn_{1-x}Sb_{15-y}$ ($x \sim 0.6$, $y \sim 0.1$). Defects in the transition metal sites were also encountered in the single crystal studies of $La_6M_{1-x}Sb_{15}$. Atom distribution, atom parameters, and occupancies, i.e., the final positional, thermal, and profile parameters, as well as the various residual values obtained from the least squares refinement, are presented in Table 2 including also interatomic distances for the next nearest neighbors within the first gap. As seen from Fig. 1 and from the residual values in Table 2, observed and calculated intensities are in fine agreement.

A.3. Formation of compounds. Room temperature X-ray Guinier patterns of samples RE_6MSb_{15} revealed a close resemblance to the pattern of homologous $Ce_6Mn_{1-x}Sb_{15}$ and were all completely indexed on the basis of an orthorhombic unit cell (see Table 1). Employing the atom parameter set derived for $Ce_6Mn_{1-x}Sb_{15}$ or La_6MSb_{15}, M = Cu, Zn, Mn, convincing agreement is found between the experimentally observed and calculated X-ray intensities confirming the isotypism with the structure type of La_6MnSb_{15}.

Particularly the cerium-containing alloys showed rather homogeneous and single phase X-ray powder patterns despite that we started from nominal compositions of Ce_6MSb_{15}, whereas the quantitative X-ray refinement arrived at a composition close to $Ce_6Mn_{0.3}Sb_{14.9}$. The discrepancy is easily explained from some substantial vapor losses during the melting as well as during the annealing procedure. In the case of Ce–Mn–Sb, phase relations indicated a composition of ca. $Ce_6Mn_{\sim 0.5}Sb_{15}$ confirming the Mn-hypostoichiometry. The series of compounds seems to be confined to representatives for La and Ce when M is either Mn or Cu. There is, however, a wide range of rare earth isotypes for RE = La, Ce, Pr, Nd, Sm, and Gd when M = Zn (see Table 1 and Fig. 2). The variation of the lattice dimensions versus the rare earths reflects the lanthanoid contraction within the RE_6ZnSb_{15} series of compounds without any particular deviation for the cerium-containing compound inferring a magnetically tripositive $^2F_{5/2}$ ground state for the Ce-atoms.

A.4. Description of the crystal structure. A three-dimensional view of the structure of Ce_6MnSb_{15} along the center line parallel [001] to the column of triangular prisms is shown in Fig. 3. In the crystal structure the antimony atoms of the positions Sb1 and Sb5 form strongly folded nets with square meshes running parallel to the plane (100). The nets are stacked in direction [100] according to the mirror plane (100). Short contacts Sb5–Sb5 ($d_{(Sb5-Sb5)}$ = 0.2831(9) nm in Ce_6MnSb_{15} to 0.2911(11) in $La_6Cu_{1.0}Sb_{15}$)

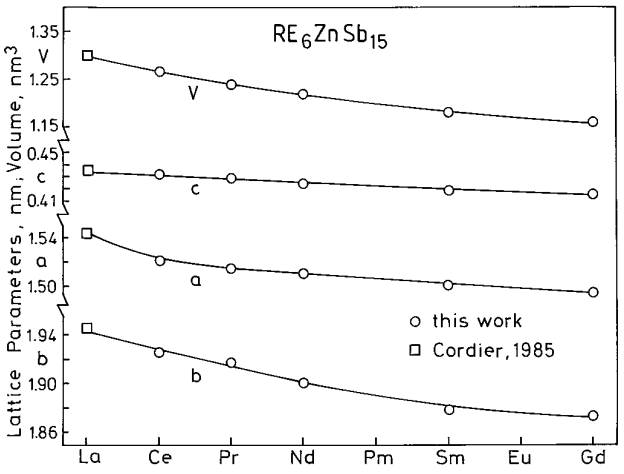

FIG. 2. Lattice parameters versus rare earth for the series RE_6ZnSb_{15}, RE = La, Ce, Pr, Nd, Sm, Gd.

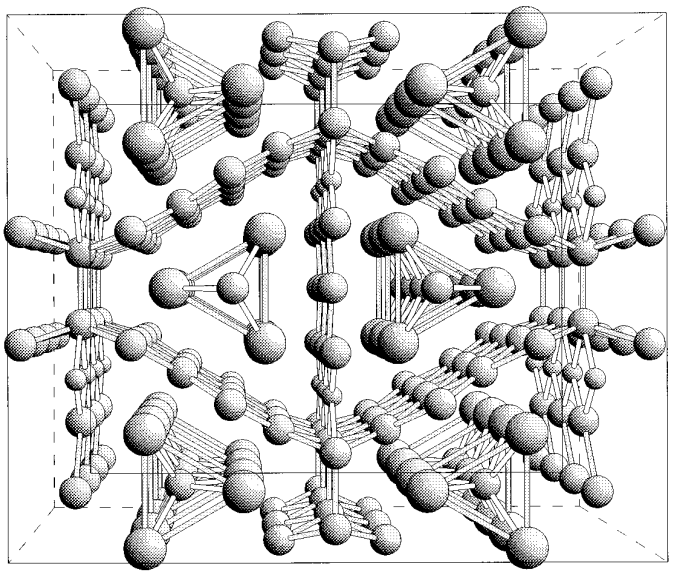

FIG. 3. Three-dimensional view of the structure of Ce_6MnSb_{15} along the center line [001] of one of the triangular prism columns. Large atoms are Ce, medium sized atoms are Sb, and small atoms are Mn.

arise in the kinks, and a three-dimensional network with large and strongly distorted hexagonal channels is formed running parallel [001]. The transition metal atoms occupy the positions opposite to the Sb–Sb bridges and reach tetrahedral coordination ($d_{(Mn-Sb)}$ = 0.2422(8) and 0.2756(7) nm in Ce_6MnSb_{15}; to 0.2451(11) and 0.2843(13) nm in La_6MnSb_{15}) by two Sb atoms, Sb5, of the square net and two additional ones of the position Sb4. The latter share common corners, thus Einereinfach chains (MSb_3) result. The Sb atoms of the common corners point to each other along the diagonal of the hexagons and are connected by a further Sb atom, Sb6, resulting in a bridge Sb4–Sb6–Sb4 ($d_{(Sb4-Sb6)}$ = 0.2992(5) and 0.3041(7) nm in La_6MnSb_{15} to 0.3041(7) and 0.3389(2) in La_6CuSb_{15}) which divides the large hexagons into two smaller ones. In these smaller channels the RE atoms form trigonal prisms sharing their basal planes and isolated Sb atoms in their centers ($d_{(Sb3-La(1,2))}$ = 0.3249(6) and 0.3269(7) nm in Ce_6MnSb_{15} to 0.3284(3) and 0.3307(2) in La_6ZnSb_{15}). The RE atoms are coordinated by 10 Sb atoms and 9 Sb and 1 M atoms, respectively. The columns of triangular prisms are enclosed in large channels built by 17 atoms in one circumference. All atoms are in layers at $z \sim 0, \frac{1}{2}$ with trigonal, quadratic, pentagonal, and hexagonal units. The coordination number of the antimony atoms ranges from 6 to 9, whereas the small M metal atoms are at the centers of distorted Sb_6 octahedra. The rather small M metal content per formula unit naturally infers an arrangement of Mn atoms with large Mn–Mn separations in favor of a high moment Mn^{2+} magnetic ground state (see Section B).

B. Magnetic Behavior of RE_6MSb_{15}, M = Mn, Zn

The magnetic susceptibilities of several single phase compounds RE_6MSb_{15} have been measured in the temperature ranges from 5 to 550 K. The results are summarized in Table 1 and Figs. 4 and 5.

For both compounds, Ce_6MnSb_{15} and Gd_6ZnSb_{15}, the onset of antiferromagnetic order due to the antiparallel alignment of the rare earth moments is encountered in the low temperature regime below T = 15 K, whereas

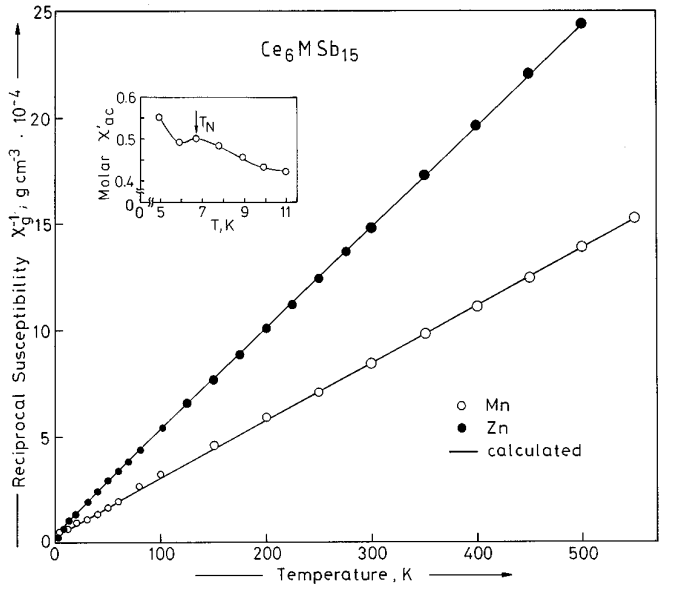

FIG. 4. Reciprocal susceptibility versus temperature for Ce_6MSb_{15}, M = Mn, Zn. Inset: Molar susceptibility versus temperature for Ce_6MnSb_{15}.

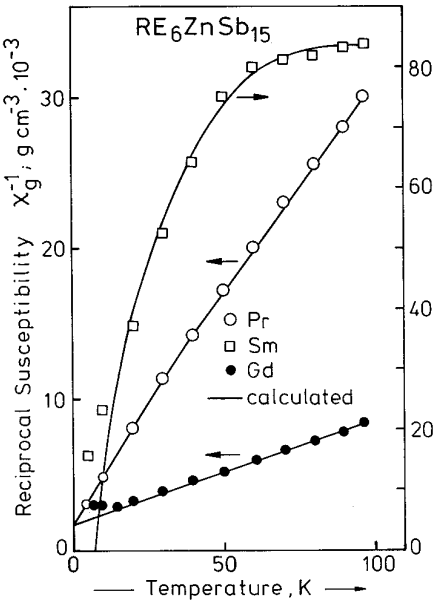

FIG. 5. Reciprocal susceptibility versus temperature for RE_6ZnSb_{15}, RE = Pr, Sm, Gd.

the remaining compounds remain in the paramagnetic state down to 5 K.

Generally the paramagnetic properties of this series of compounds obey the Curie–Weiss law. The data have been processed by a least-squares fit due to the formula

$$\chi = \frac{C}{T - \Theta p} + \chi_0,$$

where C is the Curie constant, Θ_p is the paramagnetic Curie temperature, and χ_0 is the correction due to the Pauli paramagnetism and the core diamagnetism. The calculated values of the effective moments are in good agreement with the theoretical moments of the tripositive rare earth free ion moments. For Ce_6MnSb_{15}, however, a much higher moment per formula unit is found indicating that also the manganese atom bears a magnetic moment. According to the formula $\mu_{\text{eff/f.u.}} = \sqrt{6\mu_{\text{Ce}}^2 + \mu_{\text{Mn}}^2}$, a value of 6.4 μ_B per Mn was derived suggesting a $3d^5$ ground state configuration.

The magnetic susceptibility for Sm_6ZnSb_{15} reveals a Van-Vleck-type paramagnetism of closely spaced multiplets.

ACKNOWLEDGMENTS

The authors are grateful to the Austrian National Bank for Grants 3519, 3804, and particularly for 4639. The use of the Lakeshore equipment under FWF-Grant P8218 is gratefully acknowledged.

REFERENCES

1. O. Sologub, P. Rogl, and O. Bodak, *J. Phase Equilibria*, in press.
2. G. Cordier, P. Woll, and H. Schäfer, paper P4A5, presented at the 8th Intl. Conference on Solid Compounds of Transition Elements, April 9–13, 1985.
3. P. Woll, Thesis, Technical University, Darmstadt, 1985.